Supplementary Materials

I. Experimental settings

The experimental configuration was established using the PyTorch open-source machine learning framework (https://pytorch.org). The training was conducted on a Linux operating system, utilizing a robust NVIDIA 4090 GPU with 24GB of memory. A learning rate of 0.001 was employed, with the Adam optimizer and a learning rate scheduler that reduced the learning rate by a factor of 0.1 every 70 epochs. RNA secondary structures were predicted using the RNAfold tool from the ViennaRNA package [1]. Multiple features, including Hexamer scores, Fickett scores, RNA secondary structures, and various sequence properties, were computed using R script files provided by LncFinder [2].

II. Evaluation metrics

In multi-class classification tasks, commonly used evaluation metrics include accuracy (ACC), F1-score, recall (RE), precision (PR), Area Under the ROC Curve (AUC), and Area Under the Precision-Recall Curve (AUPR). Micro-average and macro-average are two different averaging methods:

Micro-average: Calculates metrics globally by counting the total true positives, false positives, and false negatives. It is suitable when the class distribution is balanced.

Macro-average: Calculates metrics for each class separately and then takes the average. It is more appropriate for imbalanced datasets as it better reflects the performance across all classes. For imbalanced datasets, macro-average is more suitable as it better captures the performance of minority classes. Macro-average Precision (PR_macro):

$$\mathrm{PR}_{\mathrm{macro}} = \frac{1}{N}\sum_{i=1}^{N}\frac{\mathrm{TP}_i}{\mathrm{TP}_i + \mathrm{FP}_i}$$

Macro-average Recall (RE_macro):

$$\mathrm{RE}_{\mathrm{macro}} = \frac{1}{N}\sum_{i=1}^{N}\frac{\mathrm{TP}_i}{\mathrm{TP}_i + \mathrm{FN}_i}$$

Macro-average F1-score (F1_macro):

$$\mathrm{F1}_{\mathrm{macro}} = \frac{1}{N}\sum_{i=1}^{N}\frac{2 \times \mathrm{PR}_i \times \mathrm{RE}_i}{\mathrm{PR}_i + \mathrm{RE}_i}$$

Macro-average Accuracy (ACC_macro):

$$\mathrm{ACC}_{\mathrm{macro}} = \frac{1}{N}\sum_{i=1}^{N}\frac{\mathrm{TP}_i + \mathrm{TN}_i}{\mathrm{TP}_i + \mathrm{TN}_i + \mathrm{FP}_i + \mathrm{FN}_i}$$

III. Figures and Tables

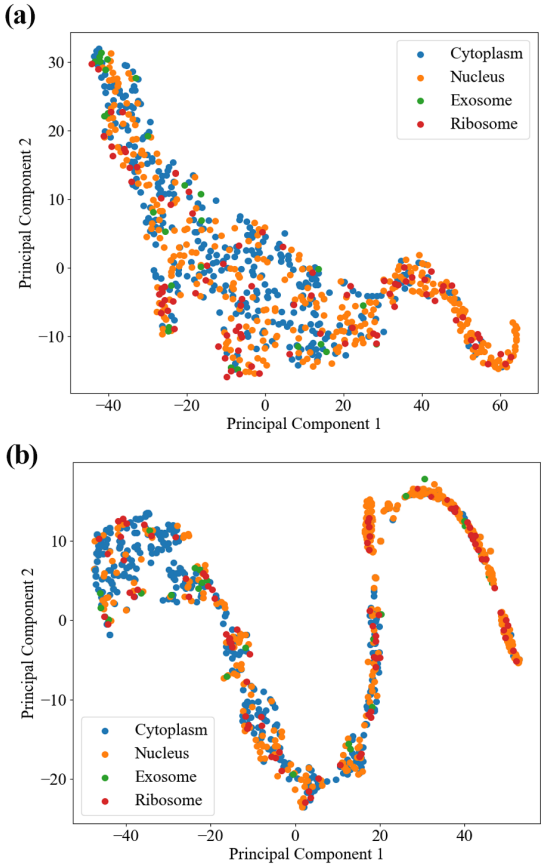

Fig. 1. Umap visualization of 6 k-mer features and multi-source lncRNA features.

TABLE I
DESCRIPTION OF MFF-LNCLOC MULTIPLE FEATURES

Feature Category	Specific Feature Name
Sequence Statistical Features	Hexamer Score
	Fickett Score
	Peak Value
	SNR
Various Properties	Seq.Nc.Dist
	Seq.Pt.Dist
	Seq.Dist.Ratio
	MFE
Secondary Structure Features	Paired-Unpaired Ratio
	Dot.Nc.Dist
	Dot.Pt.Dist
	Dot.Dist.Ratio
	SS.Nc.Dist
	SS.Pt.Dist
	SS.Dist.Ratio

TABLE II
IMPACT OF PART_NUM, PART_LEN, AND K-MER COMBINATIONS ON EXPERIMENTAL RESULTS

Methods	**ACC**	**Macro F1-score**	**Macro Recall**	**Macro Precision**	**AUC**	**AUPR**
60_64_3	0.5505	0.3770	0.38510	0.3792	0.79040	0.56260
60_64_4	0.5378	0.3717	0.37594	0.3833	0.77080	0.51242
60_64_5	0.5100	0.3663	0.37842	0.3775	0.77000	0.49576
60_64_6	0.4631	0.3057	0.31524	0.3286	0.76342	0.47126
128_64_3	0.5673	0.3782	0.38376	0.3817	0.79620	0.57698
128_64_4	0.5499	0.3754	0.38426	0.3789	0.78898	0.56158
128_64_5	0.5053	0.3806	0.40350	0.3739	0.77360	0.52470
128_64_6	0.4873	0.3300	0.33804	0.3648	0.76930	0.47938
128_128_3	0.5311	0.3589	0.36850	0.3652	0.78650	0.55754
128_128_4	0.5200	0.3983	0.41136	0.4077	0.78644	0.53660
128_128_5	0.5147	0.3898	0.38518	0.4268	0.78352	0.52236
128_128_6	0.4926	0.3550	0.35532	0.4126	0.77844	0.50822

TABLE III
EFFECT OF DIFFERENT SAMPLING PROBABILITY COMBINATIONS

	ACC	Macro F1-score	AUC
[0.25, 0.25, 0.25, 0.25]	0.5263	0.3480	0.7669
[0.15, 0.2, 0.3, 0.35]	0.5574	0.3596	0.7861
[0.15, 0.15, 0.35, 0.35]	0.5379	0.3515	0.7718
[0.2, 0.2, 0.3, 0.3]	0.5674	0.3782	0.7962

TABLE IV
EFFECT OF DIFFERENT LOSS FUNCTION

	ACC	Macro F1-score	AUC
Cross Entropy Loss	0.5368	0.3329	0.7813
Dice Loss	0.5531	0.3517	0.7917
Focal Loss	0.5674	0.3782	0.7962

IV. CASE STUDY

In this experiment, 14 sequences were involved in either suppressing or promoting tumor cell development, engaging in multiple pathways related to tumor biology and the pathogenesis of various cancers, including liver cancer. For example, LINC01270 is an oncogene in liver cancer that promotes tumor development by increasing the expression of miR-326, which in turn targets LARP1 [3]. GAS5, an effective prognostic biomarker, is known for its sensitivity and specificity in predicting immune thrombocytopenia [4]. MEG3, with its low expression, inhibits the proliferation and metastasis of glioma cells [5]. BBOX1-AS1 regulates miR-361-3p/MUC13 to suppress tumor development, presenting a potential therapeutic biomarker for prostate cancer [6]. lncRNA PVT1 promotes the proliferation, migration, and EMT process in colorectal cancer [7]. LINC01572 inhibits lung cancer cell viability, possibly regulating iron death in lung cancer [8]. lncRNA CBR3-AS1 effectively suppresses nasopharyngeal carcinoma cell growth [9]. SNHG6 interacts with BOP1 protein to accelerate glucose metabolism in colorectal cancer cells, thereby promoting cell proliferation and inhibiting apoptosis [10].

TABLE V
CASE STUDIES

ncRNA Name	**Associated Cancer**	**MFF-LncLoc Prediction**	**Verified Localization**	**Pubmed ID**
LINC01270	Lung adenocarcinoma	Nucleus	Nucleus	36694453
FOXD2-AS1	Colorectal cancer	Nucleus	Nucleus	36718294
GAS5	Immune thrombocytopenia	Cytoplasm	Cytoplasm	36731007
MEG3	Psoriasis vulgaris	Nucleus	Nucleus	36718302
BBOX1-AS1	Gastric cancer	Nucleus	Nucleus	36700475
LINC00667	Breast cancer	Cytoplasm	Cytoplasm	36700472
PVT1	Ovarian cancer	Nucleus	Nucleus	36688109
LINC01572	Lung adenocarcinoma	Nucleus	Nucleus	36686701
MALAT1	Hepatocellular carcinoma	Nucleus	Nucleus	36685103
H19	Hepatocellular carcinoma	Nucleus	Cytoplasm	36671388
LINC00473	Multiple types of cancer	Ribosome	Nucleus	36596056
CBR3-AS1	Cervical cancer	Nucleus	Nucleus	36591804
LINC00900	Liver cancer	Nucleus	Cytoplasm	36641651
SNHG6	Lung adenocarcinoma	Cytoplasm	Cytoplasm	36605586

REFERENCES

[1] R. Lorenz, S. H. Bernhart, C. Höner zu Siederdissen, H. Tafer, C. Flamm, P. F. Stadler, and I. L. Hofacker, "Viennarna package 2.0," *Algorithms for molecular biology*, vol. 6, pp. 1–14, 2011.

[2] S. Han, Y. Liang, Q. Ma, Y. Xu, Y. Zhang, W. Du, C. Wang, and Y. Li, "Lncfinder: an integrated platform for long non-coding rna identification utilizing sequence intrinsic composition, structural information and physicochemical property," *Briefings in bioinformatics*, vol. 20, no. 6, pp. 2009–2027, 2019.

[3] W. Zhang, C. Cao, J. Shen, S. Shan, Y. Tong, H. Cai, Z. Han, and H. Chai, "Long non-coding rna linc01270 is an onco-promotor in lung adenocarcinoma by upregulating larp1 via sponging mir-326," *Bioengineered*, vol. 13, no. 6, pp. 14 472–14 488, 2022.

[4] H. Hodeib, D. El Amrousy, E. Elaskary, N. Hablas, A. Youssef, and D. Abdelhai, "lncrna gas5 and runx1 genes in children with primary immune thrombocytopenia," *Journal of Pediatric Hematology/Oncology*, vol. 45, no. 3, pp. e395–e400, 2023.

[5] Z. A. Nour, Y. Elwan, Y. Nassar, M. F. Elmasry, L. Rashed, and S. S. Ashour, "Possible role of lncrna meg3-microrna-21 and endoplasmic reticulum (er) stress proteins in the pathogenesis of psoriasis vulgaris," *Reports of biochemistry & molecular biology*, vol. 11, no. 3, p. 367, 2022.

[6] T. Cai, B. Peng, J. Hu, and Y. He, "Long noncoding rna bbox1-as1 promotes the progression of gastric cancer by regulating the mir-361-3p/mucin 13 signaling axis," *Bioengineered*, vol. 13, no. 5, pp. 13 407–13 421, 2022.

[7] L. Dong, H. Wang, Y. Gao, S. Wang, and W. Wang, "Long non-coding rna pvt1 promotes the proliferation, migration and emt process of ovarian cancer cells by regulating ctgf," *Oncology letters*, vol. 25, no. 2, pp. 1–7, 2023.

[8] L. Hong, X. Wang, W. Cui, F. Wang, W. Shi, S. Yu, Y. Luo, L. Zhong, and X. Zhao, "Construction of a ferroptosis scoring system and identification of linc01572 as a novel ferroptosis suppressor in lung adenocarcinoma," *Frontiers in Pharmacology*, vol. 13, p. 1098136, 2023.

[9] C. Yi-Pin, Y. Huang, J. Zhang, L. Xiao-Li, Z. Fang, K. Zhang, X. Song-Yuan, Y. Yan, H.-W. HUANG, and G. Yu, "Lncrna cbr3-as1 predicts a poor prognosis and promotes cervical cancer progression through the mir-3163/lasp1 pathway." *Neoplasma*, vol. 69, no. 6, 2022.

[10] K. Chen, X. Wang, B. Wei, R. Sun, C. Wu, and H.-j. Yang, "Lncrna snhg6 promotes glycolysis reprogramming in hepatocellular carcinoma by stabilizing the bop1 protein," *Animal Cells and Systems*, vol. 26, no. 6, pp. 369–379, 2022.